Supplementary Information

Self-Assembling Peptide Nanomaterials Co-Engineered with Linoleic Acid and Catechol Motifs for Synergistic Ferroptosis-Photothermal-Chemotherapy

Binbin Gao,[a] Xin Tian,*[b] and Xinming Li*[a]

[a.] College of Chemistry, Chemical Engineering and Materials Science, Soochow University, Suzhou 215123, China.

[b.] State Key Laboratory of Radiation Medicine and Protection, School for Radiological and Interdisciplinary Sciences (RAD-X), Soochow University, Suzhou, 215123, China.
Email: xtian@suda.edu.cn; xinmingli@suda.edu.cn.

Contents

14. The standard curve of absorbance of DOX at different concentrations (0, 25, 50, 75, 100, and 125 μg/mL) (Fig. S17)
15. UV-vis absorbance of the LAKDCuD and LAKDFeD solutions at 480 nm (Fig. S18)
16. DOX Release from LAKDFeD in Vitro (Fig. S19)
17. The effect of pH on the catalytic oxidation of TMB by LAKDCu and LAKDFe (Fig. S20)
18. The effects of LAKDCu concentrations and reaction temperatures on the catalytic oxidation of GSH by LAKDCu (Fig. S21)
19. Flow cytometry analysis of 4T1 cells treated by free DOX and LAKDCuD for 3 and 6 h (Fig. S22)
20. Flow cytometric analysis of 4T1 cells stained by DCFH-DA (Fig. S23)
21. Flow cytometric analysis of intracellular GSH levels in 4T1 cells (Fig. S24)
22. Cell viabilities of HUVEC and L929 cells co-cultured with SAKDCu and LAKDCu for 24 h (Fig. S25)
23. Viabilities of 4T1 cells treated by varied amounts of DOX and LAKDCuD (Fig. S26)
24. Cell viability of 4T1 cells co-treated with LAKDCu and different concentrations of ferrostatin-1 (Fer-1) for 24 h (Fig. S27)

1. Materials and methods

2-chlorotrityl chloride resin, Fmoc-Ser(tBu)-OH, Fmoc-Asp(OtBu)-OH, Fmoc-Gly-OH, Fmoc-Arg(pbf)-OH, Fmoc-Lys(Boc)-OH and Fmoc-DOPA-(acetonide)-OH were purchased from Shanghai GL Biochem (Shanghai, China). Linoleic acid, stearic acid, DOX·HCl was provided by Aladdin (Shanghai, China). $CuCl_2 \cdot 2H_2O$ and $FeCl_3 \cdot 6H_2O$ were produced by Sinopharm Chemical Reagent Co. Ltd. (Shanghai, China). 3,3',5,5'-tetramethylbenzidine (TMB) and 5,5'-dithiobis-2-(nitrobenzoicacid) (DTNB) were obtained from Macklin. Hydrogen peroxide was provided by Yonghua. Ferrostatin-1 (Fer-1) was purchased from Sigma-Aldrich (USA). GSH, DCFH-DA, CCK-8 kit, Hoechst 33342, Lipid Peroxidation Assay Kit with BODIPY 581/591 C11 and LIVE/DEAD cell staining reagents and Annexin V-FITC/PI apoptosis assays kit were provided by Beyotime Co. Ltd (Shanghai, China). ThiolTrace™ Violet was from AAT Bioquest (USA). DMEM was provided by Gibco (USA). Phosphate buffer saline (PBS) was obtained from Bioind (ISR). Penicillin-streptomycin solution was obtained from Dalian Meilun biological Co. Ltd. 4T1, HUVEC and L929 cells were purchased from biobw Co. Ltd (Beijing, China). 808 nm laser (MDL-H-808 nm-5W-BH80521) was purchased from the Changchun Laser

Optoelectronics Technology Co. Ltd (China). ^{1}H NMR spectra were recorded on the Unity Inova 400 MHz by using DMSO-*d*6 as the solvent. MALDI-TOF MS analysis was conducted on a Bruker Ultraflex-Treme mass spectrometer (Germany). Transmission Electron Microscope (TEM) images were recorded on the HT7700 (Japan). UV-vis spectroscopy characterizations were performed on the Shimadzu UV1900i (Japan). Fluorescence spectra were obtained from F-2700 fluorescence spectrophotometer (Japan) and BioTek Synergy Neo microplate reader. The temperature changes were recorded by an infrared camera (Fotric 225s, China). CLSM images of cell uptake, intracellular ROS levels, intracellular GSH levels and live/dead cell staining were acquired by the confocal laser scanning microscope (CLSM, Zeiss, Germany).

2. Experimental section

2.1 Peptide synthesis: LA-KK-DOPA-GRGDS and SA-KK-Dopa-GRGDS were synthesized from corresponding amino acids by using the solid-phase peptide synthesis (SPPS) technique with the application of 2-chlorotrityl chloride resin (100-200 mesh and 1.3-1.8 mmol/g). Briefly, 0.5 g 2-chlorotrityl chloride resin was swelled in dry dichloromethane (DCM) with constant nitrogen gas bubbling for 30 min and then was washed by dry dimethylformamide (DMF) five times. Afterward, the solution containing Fmoc-Ser(tBu)-OH and *N,N*-diisopropylethylamine (DIEA) in DMF was added. After reaction for 1.5 h, the resin was rinsed by dry DMF four times and quenched by the blocking solution (32:6:2 of DCM/methanol/DIEA) for 10 min twice. Then, the resin was treated with 20% piperidine in DMF for 30 min and washed thoroughly with DMF four times. To couple the next amino acid to the free amino group, O-(Benzotriazol-1-yl)-*N,N,N',N*'-tetramethyluronium hexafluorophosphate (HBTU) was used as coupling reagent. The growth of the peptide chain was according to the established Fmoc SPPS protocol. Ultimately, the synthetic peptide was cleaved from the resin by using cleavage cocktail (TFA: H_2O=95:5). The final yield of LA- KK-DOPA-GRGDS and SA-KK-DOPA-GRGDS peptide were about 70%.

LA-KK-DOPA-GRGDS: ^{1}H NMR (400 MHz, DMSO) δ 8.68 (s, 1H), 8.45 (s, 1H), 8.34 (s, 2H), 8.22 – 8.08 (m, 2H), 7.97 (d, J = 6.5 Hz, 1H), 7.73 (s, 4H), 7.22 (s, 2H), 6.66 (s, 1H), 6.58 (s, 1H), 6.48 (s, 1H), 5.54 – 5.22 (m, 2H), 5.06 (s, 1H), 4.61 (dd, J = 13.2, 7.8 Hz, 1H), 4.43 – 4.10 (m, 6H), 3.83 – 3.59 (m, 7H), 3.08 (s, 2H), 2.72 (ddd, J = 33.3, 19.9, 10.8 Hz, 8H), 2.22 – 1.85 (m, 7H), 1.80 – 1.60 (m, 5H), 1.55 – 1.44 (m, 9H), 1.38 – 1.35

(m, 1H), 1.24 (s, 20H), 1.10 (t, J = 7.0 Hz, 3H), 0.85 (d, J = 7.0 Hz, 3H). MS: calcd M= 1187.69, obsd $[M + H]^+$=1188.618.

SA-KK-DOPA-GRGDS: ^{1}H NMR (400 MHz, DMSO) δ 8.69 (d, J = 19.4 Hz, 2H), 8.28 – 8.20 (m, 2H), 8.00 (dd, J = 32.3, 7.4 Hz, 3H), 7.83 (d, J = 7.5 Hz, 1H), 7.67 (s, 4H), 7.56 (s, 1H), 6.61 (dd, J = 10.0, 4.8 Hz, 2H), 6.47 (d, J = 8.1 Hz, 1H), 4.97 (s, 1H), 4.67 (dd, J = 13.1, 8.0 Hz, 1H), 4.41 – 4.17 (m, 5H), 3.76 – 3.62 (m, 6H), 3.10 (d, J = 5.4 Hz, 2H), 2.90 – 2.81 (m, 2H), 2.77 – 2.63 (m, 6H), 2.14 – 1.93 (m, 3H), 1.54 (d, J = 43.1 Hz, 14H), 1.24 (s, 36H), 0.85 (d, J = 7.0 Hz, 3H).MS: calcd M=1191.72, obsd $[M + H]^+$=1192.919, obsd $[M + Na]^+$=1214.923.

2.2 Preparation of self-assembled nanostructures from LAKD, LAKDFe, LAKDCu, SAKD and SAKDCu: 2 mg of samples were dissolved in ultrapure water and sonicated to ensure complete dissolution. Then, 48 μL of the freshly prepared solution of $CuCl_2 \cdot 2H_2O$ or $FeCl_3 \cdot 6H_2O$ (6 mg/mL) was added to each sample. The pH of the solutions was adjusted to 7.4 with 1M HCL and NaOH, and the mixed solutions were stirred uniformly at room temperature for 12 h. Then solutions were transferred to dialysis bag (MWCO:1000) and dialyzed until complete, yielding the desired solutions containing self-assembled nanostructures.

2.3 TEM characterizations: 4 μL of each sample solution were placed on a carbon-coated copper grid, and then stained with phosphotungstic acid (2.0% w/v) for 12 min. After air-drying, the nanostructures were visualized by the transmission electron microscope (Hitachi HT7700).

2.4 FTIR characterization: LAKD, SAKD, LAKDFe, LAKDCu and SAKDCu solid powders were removed and placed on the sample table and scanned by Fourier transform infrared spectrometer (FITR) with a scanning resolution of 2 cm^{-1}. The scanning range is 4000-500 cm^{-1}, and the number of scans is 64 times, removing the air background. The sample is then tested spectroscopically.

2.5 Dynamic diameter, hydrodynamic size distribution and Zeta potential measurement of self-assembled nanostructures: The 200 μL sample solution was placed in a quartz cuvette with the same light on both sides, and the particle size, dispersion index (PDI) and Zeta potential of the sample were measured by dynamic light scattering (DLS).

2.6 Photothermal properties of LAKDCu and LAKDFe: 200 μL of LAKDCu/LAKDFe solution was added into the 96-well plate and irradiated with 808 nm NIR laser for 8 min. The temperature changes were monitored by an infrared camera (Fotric 225s, China). The

photothermal conversion efficiency (η) of the LAKDCu/LAKDFe was determined according to the following equation:

$$\eta = \frac{hS(T_{max} - T_{surr}) - Q_s}{I(1 - 10^{-A_\lambda})}$$

In this equation, T_{max} means the highest temperature. T_{surr} is the average temperature of ambient and Q_s is the heat lost to the surroundings. I stands for the power density of laser and A_λ represents the absorbance value of LAKDCu at the wavelength of 808 nm. hS was calculated according to the following equation:

$$hS = \frac{mC_{H2O}}{\tau_s}$$

In this equation, m is the mass of the solution. C_{H2O} is the specific heat capacity of water. τ_s is the time constant which can be calculated according to the following equation:

$$t = -\tau_s In\theta = -\tau_s In\left(\frac{T - T_{surr}}{T_{max} - T_{surr}}\right)$$

In this equation, t denotes the time in the cooling process. θ refers to the thermal drive constant. T is the real-time temperature of time.

2.7 The payload and encapsulation efficiency of DOX within LAKDCuD/LAKDFeD: 2 mg of LAKD was dissolved in ultrapure water, fully dissolved by ultrasound, and then 48 μL or 37 μL of the freshly prepared solution of $CuCl_2 \cdot 2H_2O$ or $FeCl_3 \cdot 6H_2O$ (6 mg/mL) was added to each sample, together with 2 mg DOX, adjust the pH of the solution to 7.4 with 1M HCL and NaOH solution, and stir away from light for 24 h. The solution is then transferred to a dialysis bag (MWCO: 1000) and the required solution is obtained after the dialysis is complete.

The payload and encapsulation efficiency of DOX within LAKDCu/LAKDFe was determined according to the following equation:

$$\text{payload (\%)} = \frac{DOX\ mass\ of\ the\ load}{Quality\ of\ DOX\ input}$$

$$\text{encapsulation efficiency (\%)} = \frac{DOX\ mass\ of\ the\ load}{Carrier\ quality\ +\ DOX\ mass\ of\ the\ load}$$

2.8 DOX release in vitro: DOX was released from LAKDCuD/LAKDFeD using a dialysis-based approach, and the whole process was performed away from light due to the fluorescence of DOX. 1 mL of LAKDCuD/LAKDFeD solution was sealed in a dialysis bag (MWCO:1000) and then immersed in 10 mL of PBS buffers of different pH values

(pH 5.0, 6.5, and 7.4) for drug release in an oscillating incubator at 37°C and 100 rpm. At a predetermined time point, 1 mL of solution was removed and PBS buffer solution with the same pH and volume was added. The light group irradiated 808 nm NIR light with a laser intensity of 1.0 W/cm^2 for 8 min. Finally, the DOX solution released within 36 h was tested by UV-1900i.

$$E_r = \frac{V_e \sum_{1}^{n-1} C_i + V_0 C_n}{m_{drug}}$$

E_r represents the cumulative release of DOX; V_e represents the volume of replacement solution. C_i represents the concentration of DOX at the i time of sampling. V_0 represents the total volume of the releasing medium; C_n represents DOX concentration in the sample. n is the number of times the solution is replaced; m_{drug} represents the mass of DOX in drug-carrying nanoparticles.

2.9 Determination of catalytic activity: The peroxide-like catalytic activity of LAKDCu was detected with 3,3',5,5' -tetramethylbenzidine (TMB) as substrate in the presence of H_2O_2. 10 μL of TMB solution (40 mM) and 20 μL H_2O_2 were added to 920 μL PBS buffer (pH=5.0), mixed evenly by vortex, and then 50 μL of LAKDCu complex (6 mM) was added to initiate the reaction. The light group irradiated 808 nm NIR light with a laser intensity of 1.0 W/cm^2 for 8 min, and the absorbance of the reaction product oxTMB at 650 nm was detected by UV-1900i. Then the effects of LAKDCu concentration (0.1, 0.2, 0.3 and 0.4 mM) and reaction temperature (25, 37 and 60 °C) on the catalytic system were evaluated.

2.10 ESR analysis: The ·OH level was quantified using an electron spin resonance (ESR) spectrometer using DMPO (5, 5-dimethyl-1-pyrrolin-n-oxide) as a spin trap. In order to detect the DMPO-·OH signal, 50 μL LAKDCu (6 mM) and 20 μL H_2O_2 were mixed in PBS (920 μL, pH=5.0) in the light group (808 nm, 1.0 W/cm^2, 8 min), and DMPO (10 μL, 1M) was added rection for 10 min, ESR spectroscopic determination in quartz capillary tubes. The conditions for measuring ESR spectrum are as follows: microwave power: 1 mW, Sweep Width: 326 ± 5 mT, Mod Width: 0.1 mT, Amplitude: 600.

2.11 UV spectroscopy for measuring lipid peroxidation within LAKDCu: The degree of lipid peroxidation induced by LAKDCu was evaluated by measuring the characteristic absorption peak of conjugated dienes at 234 nm in the aqueous solution. H_2O_2 (2 mM)

was mixed with LAKD (0.3 mM), LAKDCu (0.3 mM) and SAKDCu (0.3 mM) respectively. The samples were incubated at room temperature for 20 min, and then the absorbance of the reaction products in the wavelength range of 200 - 400 nm was scanned by using a UV-Vis spectrophotometer (UV-1900i).

2.12 Fluorescence spectroscopy characterization of lipid peroxidation mediated by LAKDCu: DCFH solution (40 μM) was added to the following groups of solutions: PBS (blank control), LAKDCu (0.3 mM), SAKDCu (0.3 mM), LAKDCu (0.3 mM) +H_2O_2 (2 mM), SAKDCu (0.3 mM) +H_2O_2 (2 mM), the final volume of each group was adjusted to 1 mL. The final concentration of DCFH was 0.4 μM. 1 mL of the mixture was taken into the fluorescence colorimetric dish, and the fluorescence intensity of DCF was measured by fluorescence spectrometer at 0, 5, 10, 15, 20, 25, 30, 35, 40, 45 and 50 min respectively (DCF: E_x=480 nm, E_m=525 nm).

2.13 Characterization of GSH consumption: 10 μL of GSH solution (20 mM) and 50 μL of LAKDCu (6 mM) were added to 890 μL of PBS buffer (pH=5.0). After reaction for a specific time, 50 μL of DTNB (10 mM) was added and the absorbance at 412 nm is then monitored by using an ultraviolet-visible spectrophotometer (UV-1900i). Under the same conditions, the effect of LAKDCu on the catalytic system was evaluated by changing the reaction time (0, 1, 3, 5, 7 and 9 min), reaction temperature (25, 37 and 60°C) and concentration (0, 0.1, 0.2 and 0.3 mM).

2.14 In vitro cellular uptake: 4T1 cells were seeded in glass bottom cell culture dishes at a density of 1.2×10^5 cells/well overnight. Then the cells treated by DOX (3.27 μg/mL) and LAKDCuD (100 μg/mL) for 3 and 6 h. After that, the 4T1 cells were stained with Hoechst33342（10 μg/mL）for 20 min and washed by PBS 3 times. Finally, the cells were observed by confocal laser scanning microscopy (DOX: E_x=480 nm, E_m=570 nm; Hoechst33342: E_x=346 nm，E_m=460 nm).

4T1 cells were seeded in 6 well-plates at a density of 1.2×10^5 cells/well overnight. Then DOX and LAKDCuD were incubated with cells at the DOX concentration of 3.27 μg/mL for 3 and 6 h. After incubation, the medium was discarded, digested with trypsin, centrifuged, the supernatant was discarded, washed with PBS for 3 times, centrifuged for 4 min at 800 rpm, and then suspended with 500 μL of cold PBS. Finally, the cells were counted by flow cytometry.

2.15 Intracellular reactive oxygen species (ROS) detection: 4T1 cells were inoculated into a confocal laser culture dish with a density of 1.2×10^5 cells per well and cultured in a

constant temperature incubator (37℃，5% CO_2). Then DMEM media containing DOX (3.27 μg/mL), SAKDCu (100 μg/mL), LAKDCu (100 μg/mL) and LAKDCuD (100 μg/mL) were added and cultured for 6 h. During this period, 808 nm near-infrared laser irradiation was performed (1.0 W/cm^2, 8 min). The culture medium was removed and washed with PBS, and then 1 μL of DCFH-DA (10 mM) working liquid was added to each well, and incubated at 37℃ for 30 min in dark. After staining, the cells were washed again with PBS, and the cells were observed by confocal laser scanning microscope. The ROS production in the cells was quantitatively analyzed by flow cytometry. (DCF: E_x=480 nm, E_m=525 nm).

2.16 Intracellular GSH detection: 4T1 cells were inoculated into a confocal laser culture dish with a density of 1.2×10^5 cells per well and cultured in a constant temperature incubator (37℃，5% CO_2). Then DMEM media containing DOX (3.27 μg/mL), SAKDCu (100 μg/mL), LAKDCu (100 μg/mL) and LAKDCuD (100 μg/mL) were added and cultured for 6 h. During this period, 808 nm near-infrared laser irradiation was performed (1.0 W/cm^2, 8 min). The culture medium was removed and washed with PBS, and then 10 μL of ThiolTracker^{TM} Violet (2 mM) working liquid was added to each well, incubated at 37℃ for 30 min in dark light, and washed again with PBS after dyeing. The cells were observed by confocal laser scanning microscope and the GSH levels were quantitatively analyzed by flow cytometry. (E_x=405 nm, E_m=525 nm).

2.17 Intracellular lipid peroxide (LPO) detection: 4T1 cells were inoculated into a confocal laser culture dish with a density of 1.2×10^5 cells per well and cultured in a constant temperature incubator (37℃，5% CO_2). Then DMEM media containing DOX (3.27 μg/mL), SAKDCu (100 μg/mL), LAKDCu (100 μg/mL) and LAKDCuD (100 μg/mL) were added and cultured for 6 h. During this period, 808 nm near-infrared laser irradiation was performed (1.0 W/cm^2, 8 min). The culture medium was removed and washed with PBS, then 2.5 μL of C11-BODIPY 581/591 (2 mM) working solution was added to each well, and incubated at 37℃ without light for 30 min. After staining, the cells were washed again with PBS, and the cells were observed by confocal laser scanning microscope. (E_x=488 nm, E_m =510 nm).

2.18 Western blot assays of intracellular GPX4: 4T1 cells were seeded into 6-well plates at a density of 1.2×10^5 cells per well. After 12 h of culture, DOX (3.27 μg/mL), LAKDCu (100 μg/mL), and LAKDCuD (100 μg/mL) were added to the culture medium. During this period, 808 nm near-infrared laser irradiation was performed (1.0 W/cm^2, 8 min).

After 24 h of incubation, the cells were carefully rinsed twice with PBS. Then, the 4T1 cells were collected and lysed in a universal lysis buffer. Total protein was quantified using a BCA protein assay kit, and the total protein concentration was adjusted to be consistent among groups. Target proteins were separated by SDS-PAGE and transferred to PVDF membranes. After blocking with 5% skim milk buffer for 1 h, the proteins on the polyvinylidene fluoride membranes were incubated overnight at 4°C with GPX4 primary antibody (1:1000 dilution), followed by incubation with secondary antibody at room temperature for 1 h. GAPDH protein (1:1000 dilution) was used as a loading control. The corresponding secondary antibodies were further incubated to detect enhanced chemiluminescence**.**

2.18 Cell compatibility: HUVEC cells and L929 cells were inoculated into 96-well plates with a density of 8×10^3 cells per well, and cultured in a constant temperature incubator (37℃，5% CO_2) for 24 h. After the culture medium was removed, DMEM medium containing different concentrations of SAKDCu and LAKDCu (0, 25, 50, 100, 150, 200 and 300 μg/mL) was added and incubated for 24 h. Then the medium in the pore plate was discarded, followed by the addition of 100 μL of medium solution with 10% CCK-8 and staining for 30 min under light protection. The absorbance value was measured at 450 nm using a multifunctional enzyme marker, and the cell survival rate was calculated.

2.19 In vitro cytotoxicity test: The cytotoxicity of DOX, SAKDCu, LAKDCu and LAKDCuD to 4T1 cells was evaluated by CCK-8 assay. 4T1 cells were inoculated into 96-well plates with a density of 8×10^3 cells per well, and cultured in a constant temperature incubator (37℃，5% CO_2) for 24 h. After the culture medium was removed, DMEM medium containing DOX, SAKDCu, LAKDCu and LAKDCuD in different concentrations were added and incubated for 24 h. During this period, 808 nm near-infrared laser irradiation was performed (1.0 W/cm^2, 8 min). Untreated cells were used as controls. Then the medium in the pore plate was discarded, followed by the addition of 100 μL of medium solution with 10% CCK-8 and staining for 30 min under light protection. Then the absorbance value was measured at 450 nm using a multifunctional enzyme marker, and the cell survival rate was calculated.

2.20 Live/dead assay: Live/dead staining was performed by using the Calcein AM/PI staining kit. 4T1 cells were inoculated into confocal laser culture dish with a density of 1.5×10^5 cells per well and cultured in a constant temperature incubator (37℃，5% CO_2) for 24 h. Then DMEM media containing DOX (3.27 μg/mL), SAKDCu (100 μg/mL),

LAKDCu (100 μg/mL) and LAKDCuD (100 μg/mL) were added and cultured for 24 h. During this period, 808 nm near-infrared laser irradiation was performed (1.0 W/cm^2, 8 min). Then, 1 μL of calcein (4 mM) and 5 μL of PI (1.5 mM) were added to each petri dish and placed in a constant temperature incubator (37℃，5% CO_2) for 15 min without light. After staining, the cells were observed by confocal laser microscopy (Caicein-Am: E_x=490 nm, E_m=515 nm; PI: E_x=488 nm, E_m=630 nm).

2.21 Cell apoptosis assay: Apoptosis of 4T1 cells was measured using Annexin V-FITC apoptosis detection kit. 4T1 cells were inoculated into 6-well plates with a density of 1.5×10^5 cells per well and cultured in a constant temperature incubator (37℃，5% CO_2) for 24 h. Then DMEM media containing DOX (3.27 μg/mL), SAKDCu (100 μg/mL), LAKDCu (100 μg/mL) and LAKDCuD (100 μg/mL) were added and cultured for 24 h. During this period, 808 nm near-infrared laser irradiation was performed (1.0 W/cm^2, 8 min). Then the culture medium was collected and washed once with PBS, digested with trypsin solution, centrifuged at 1200 rpm for 5 min, and then re-suspended in 500 μL of Annexin V-FITC binding buffer. The cells were incubated with 5 μL of Annexin V-FITC and 10 μL of PI for 15 min and the sample was analyzed by flow cytometry.

3. Synthesis and characterizations of LA-KK-DOPA-GRGDS and SA-KK-DOPA-GRGDS

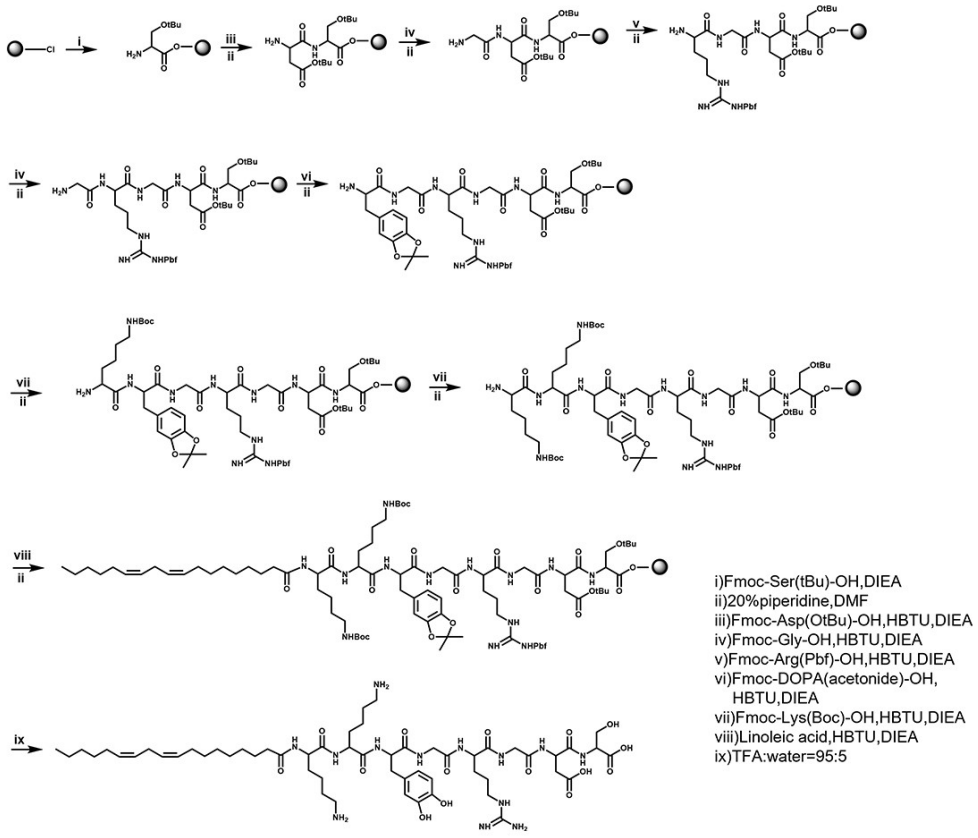

Fig. S1. Synthetic routes for the preparation of LA-KK-DOPA-GRGDS.

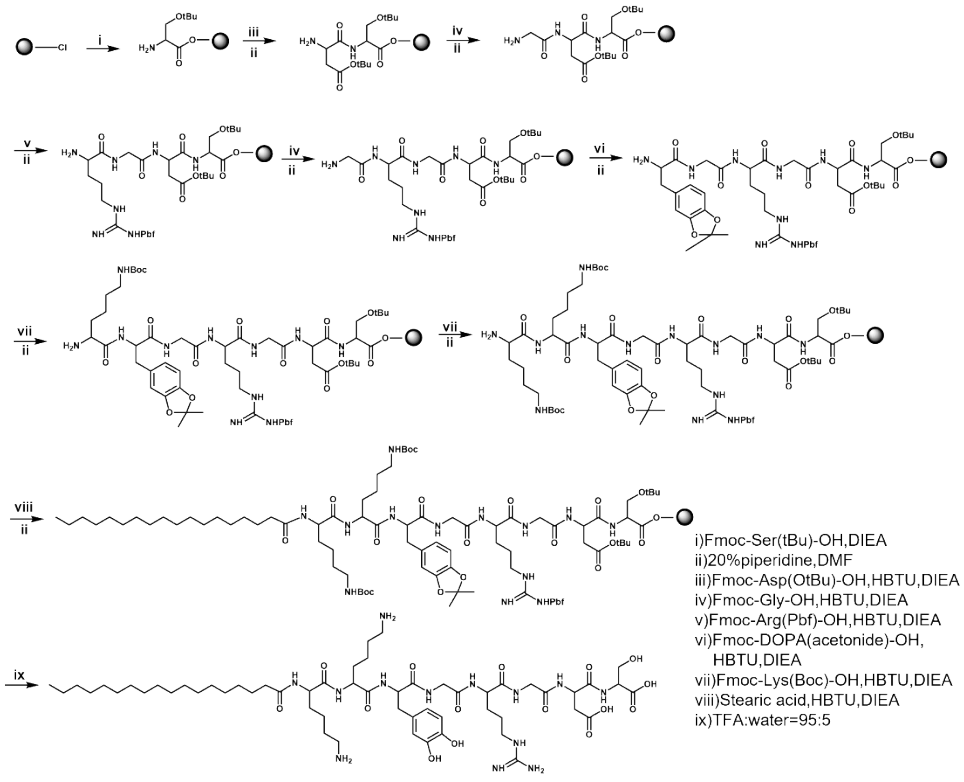

Fig. S2. Synthetic routes for the preparation of SA-KK-DOPA-GRGDS.

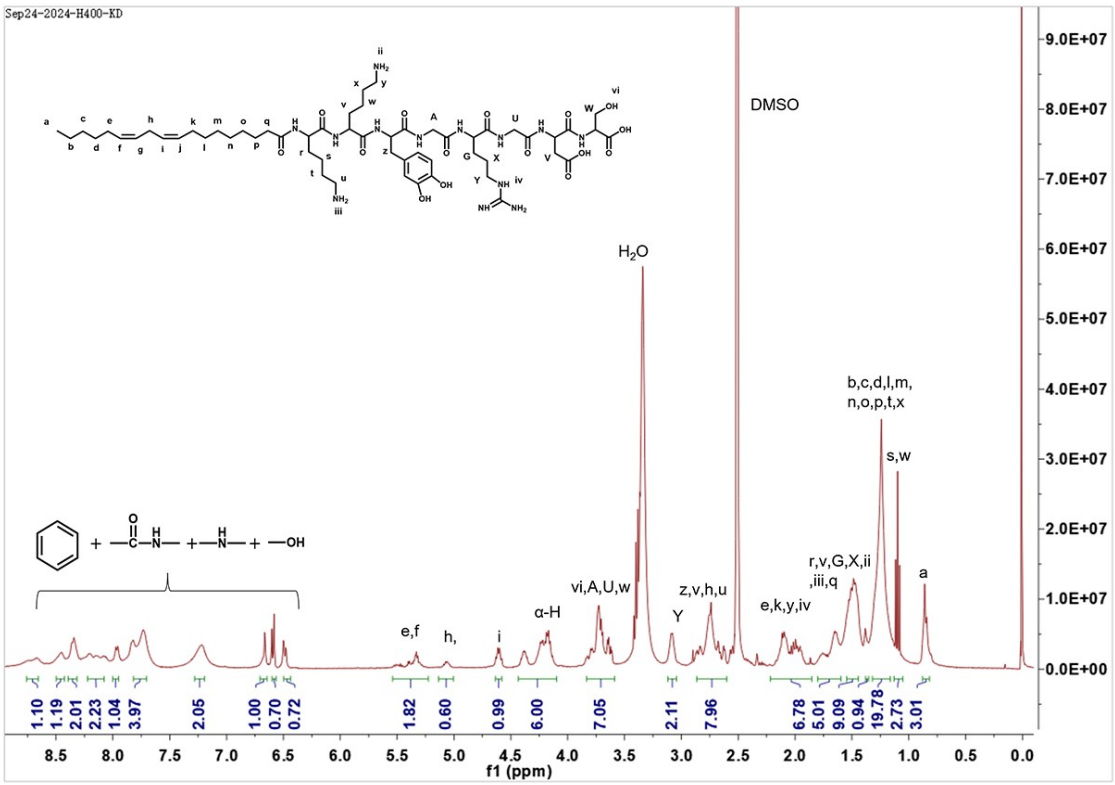

Fig. S3. [1]H NMR of LA-KK-DOPA-GRGDS in DMSO-*d6*.

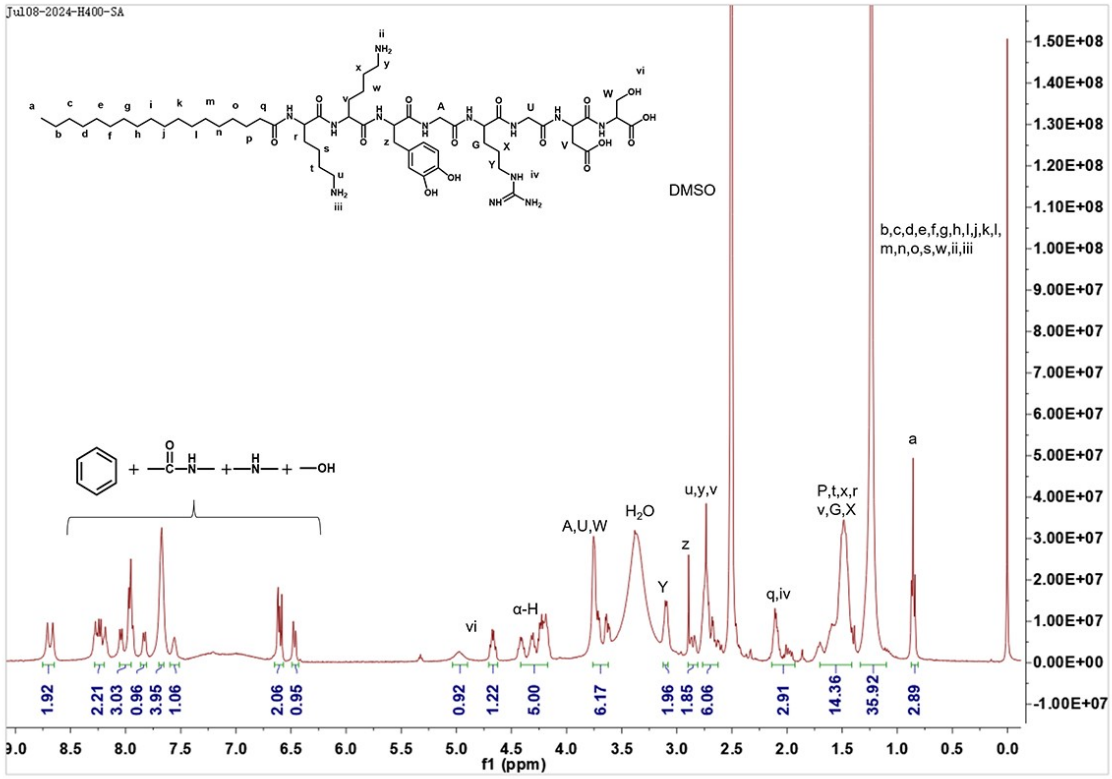

Fig. S4. [1]H NMR of SA-KK-DOPA-GRGDS in DMSO-*d6*.

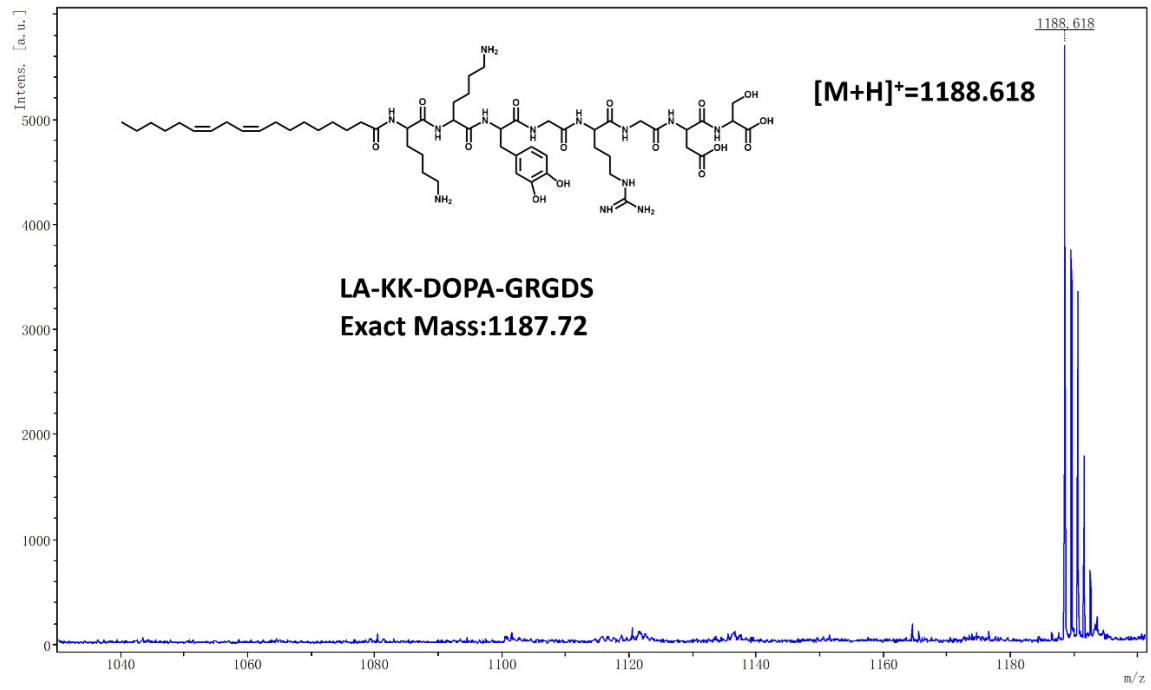

Fig. S5. MALDI-TOF MS of LA-KK-DOPA-GRGDS.

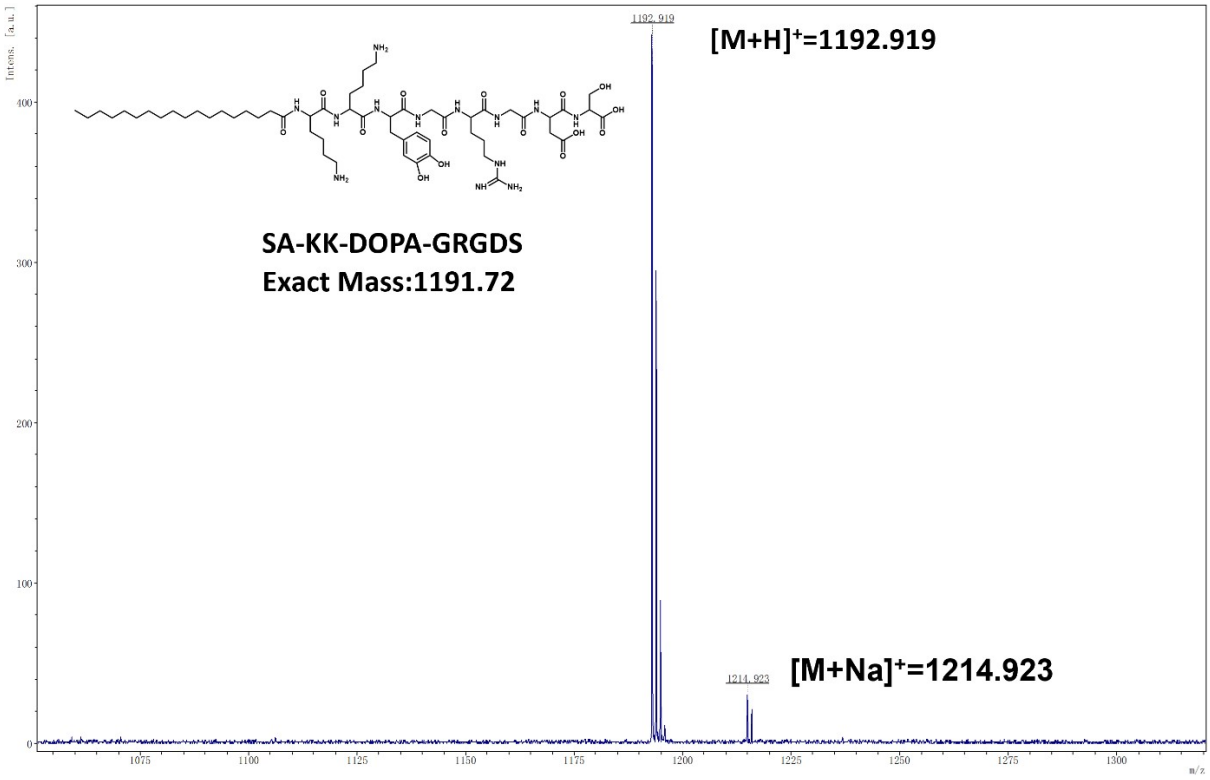

Fig. S6. MALDI-TOF MS of SA-KK-DOPA-GRGDS.

4. TEM characterization of self-assembled nanostructures of SAKD, SAKDCu and LAKDCuD

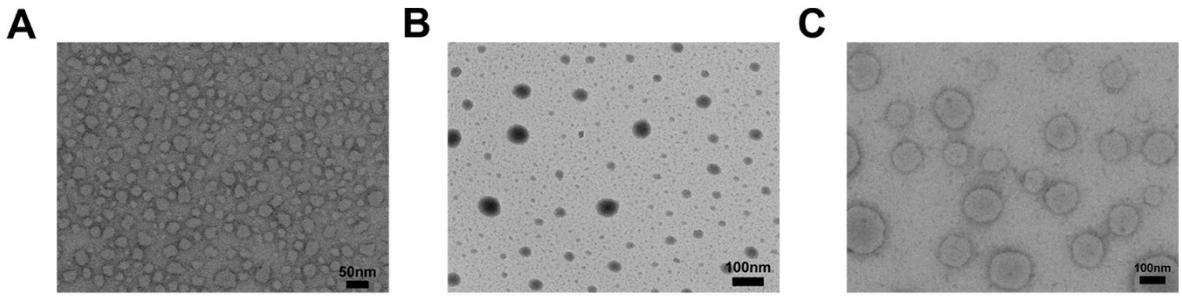

Fig. S7. TEM images of self-assembled nanostructures of (A) SAKD, (B) SAKDCu and (C) LAKDCuD (0.2 wt%, pH=7.4).

5. pH- and laser-responsive properties of LAKDCuD

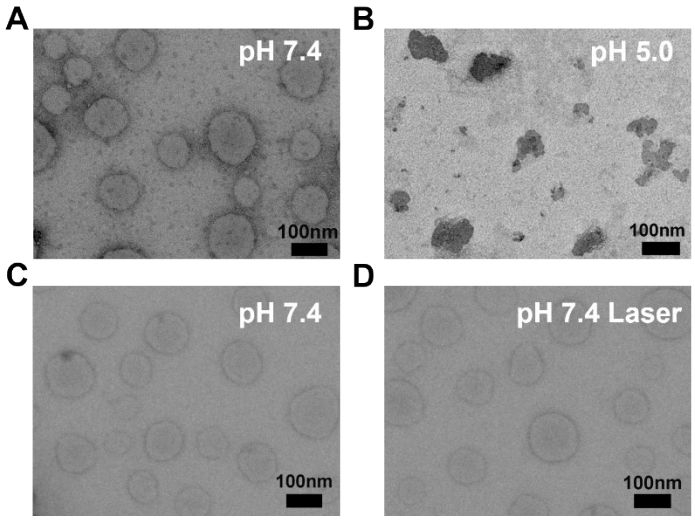

Fig. S8. TEM images of LAKDCuD (A) at pH 7.4 and (B) pH 5.0 TEM images of LAKDCuD (C) before and (D) after 808 nm irradiation (1.0 W/cm^2, 8 min).

6. FTIR characterization of self-assembled nanostructures of SAKD and SAKDCu

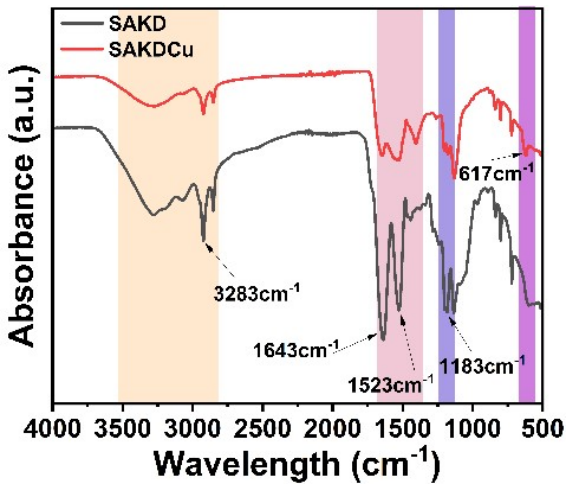

Fig. S9. FTIR spectra of self-assembled nanostructures of SAKD and SAKDCu.

7. Dynamic diameters and hydrodynamic size distributions of self-assembled nanostructures of SAKD, SAKDCu and LAKDCuD determined by DLS

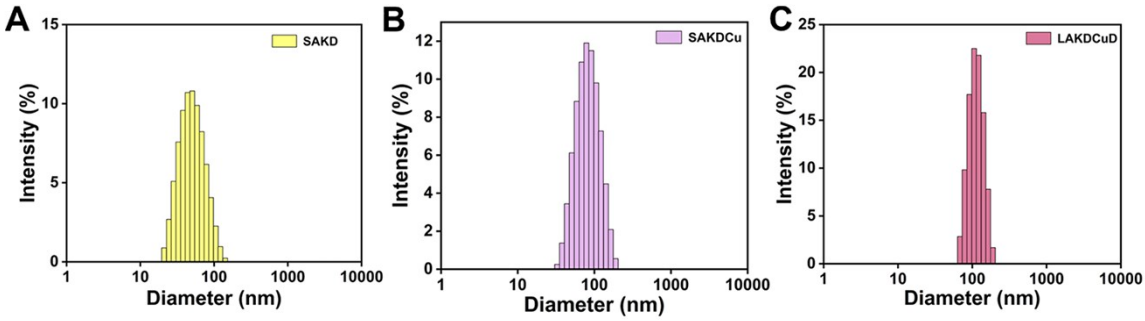

Fig. S10. The dynamic diameter and hydrodynamic size distributions of self-assembled nanostructures of (A) SAKD, (B) SAKDCu and (C) LAKDCuD shown in Fig.S7.

8. Zeta potentials of self-assembled nanostructures of SAKD, SAKDCu and LAKDCuD

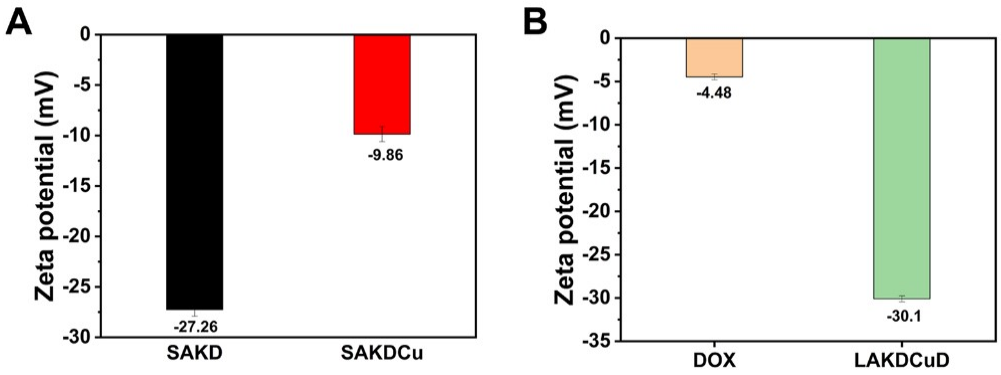

Fig. S11. Zeta potentials of self-assembled nanostructures of (A) SAKD and SAKDCu, (B)DOX and LAKDCuD.

9. Stabilities of the solutions of LAKDFe, LAKDCu, SAKDCu and LAKDCuD

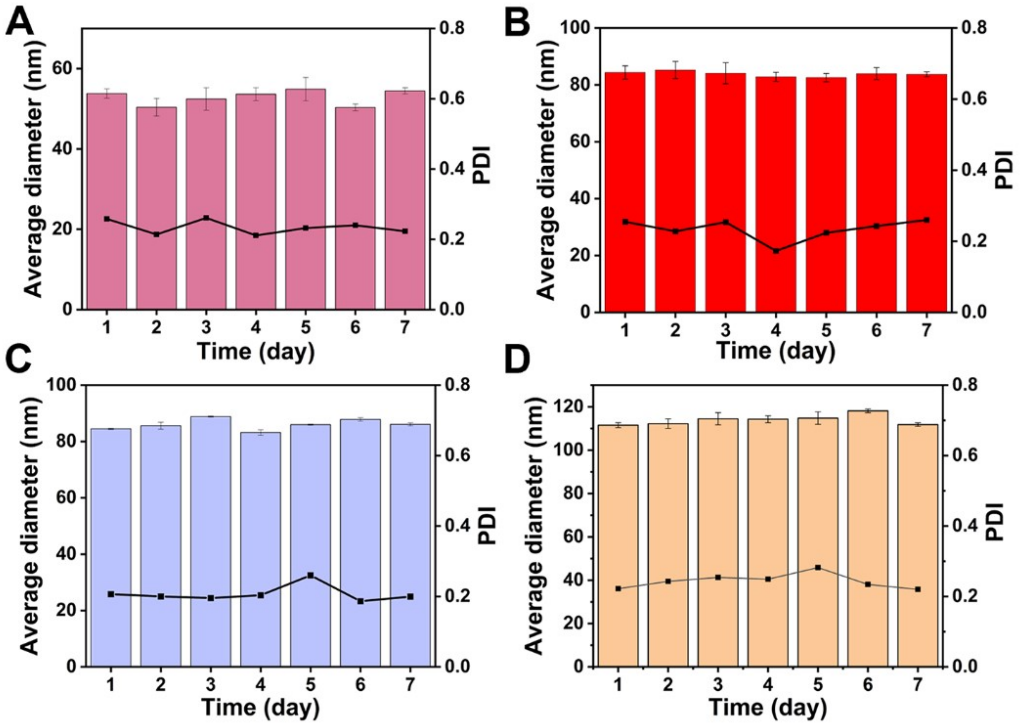

Fig. S12. The hydrodynamic size and PDI of the self-assembled nanostructures (A) LAKDFe, (B) LAKDCu, (C) SAKDCu and (D) LAKDCuD by DLS over a period of 7 days.

10. Photographs of the solutions containing LAKD, LAKDFe and LAKDCu (2 mg/mL, pH=7.4)

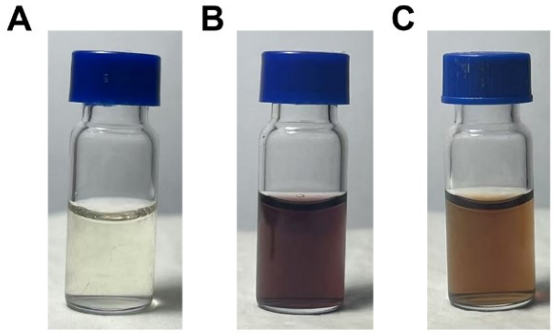

Fig. S13. Photoimages of the solutions of (A) LAKD, (B) LAKDFe and (C) LAKDCu (2 mg/mL, pH=7.4).

11. Photographs of the solutions of LAKDFe and LAKDCu containing EDTA, Triton X-100 or urea

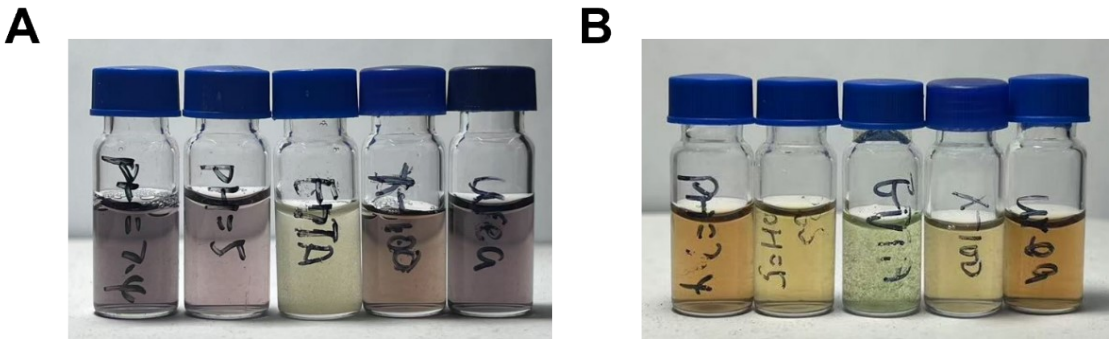

Fig. S14. Photographs of the (A) LAKDFe (0.85 mM) and (B) LAKDCu (0.85 mM) solution containing EDTA (20 mM), Triton X-100 (20 mM) or urea (20 mM).

12. The absorbance of the LAKDCu/LAKDFe solutions in the NIR region

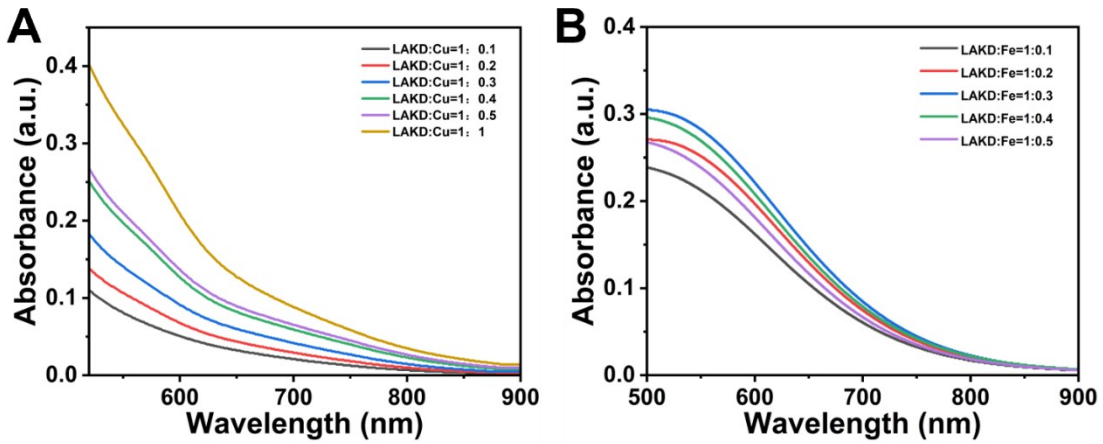

Fig. S15. (A) The absorbance of LAKDCu with different peptide/Cu^{2+} feeding ratios (1:0.1, 1:0.2, 1:0.3, 1:0.4, 1:0.5 and 1:1) in the NIR region. (B) The absorbance of LAKDFe with different peptide/Fe^{3+} feeding ratios (1:0.1, 1:0.2, 1:0.3, 1:0.4 and 1:0.5) in the NIR region

13. Photothermal Properties of LAKDFe

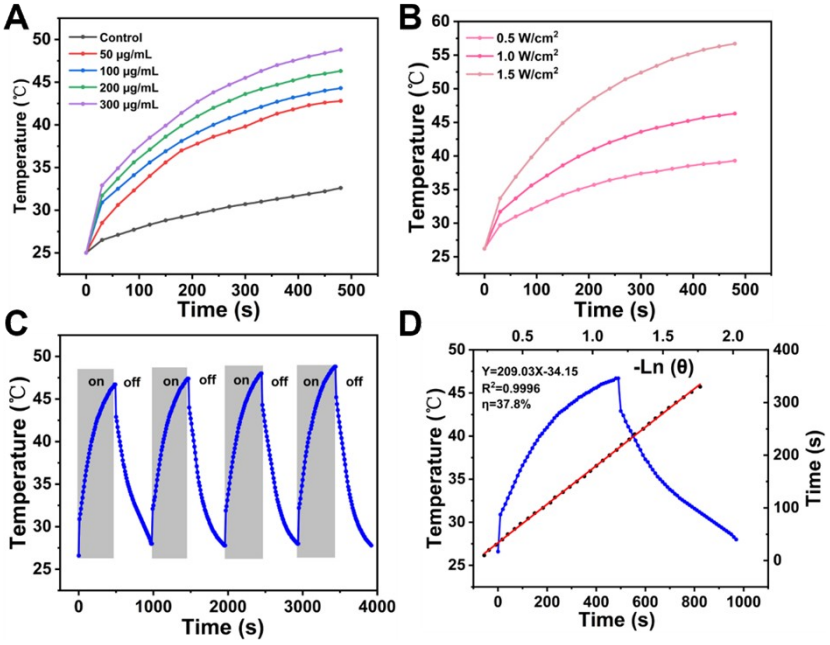

Fig. S16. (A) Photothermal effect of LAKDFe at different concentrations (50, 100, 200 and 300 μg/mL) under 808 nm laser irradiation (1.0 W/cm^2) for 8 min. (B) Photothermal performance of LAKDFe (200 μg/mL) under 808 nm laser irradiation with different light power densities (0.5, 1.0 and 1.5 W/cm^2) for 8 min. (C) Photothermal stability of LAKDFe under four on/off cycles of irradiation at 808 nm (1.0 W/cm^2). (D) Heating and cooling curves of LAKDFe under 808 nm laser irradiation, and the linear relationship between the cooling period and -lnθ.

14. The standard curve of DOX absorbance at different concentrations

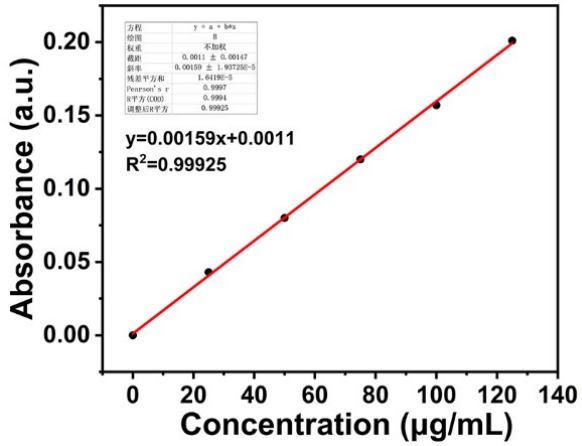

Fig. S17. The standard curve represents the relationship between the concentrations of DOX in solutions (0, 25, 50, 75, 100 and 125 μg/mL) and the corresponding absorbance at 480 nm.

15. UV-vis absorbance of the LAKDCuD and LAKDFeD solutions at 480 nm

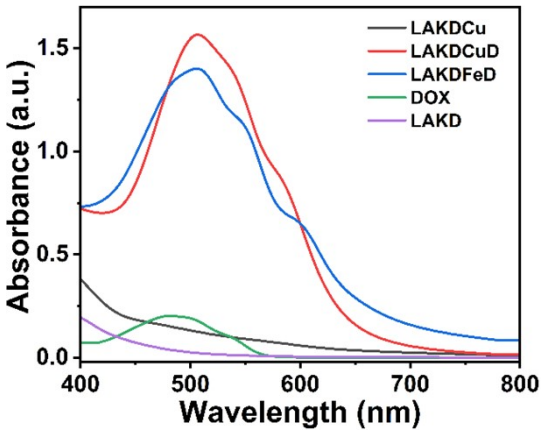

Fig. S18. UV-vis absorption of the LAKDCuD and LAKDFeD solutions at 480 nm.

16. DOX Release from LAKDFeD in Vitro

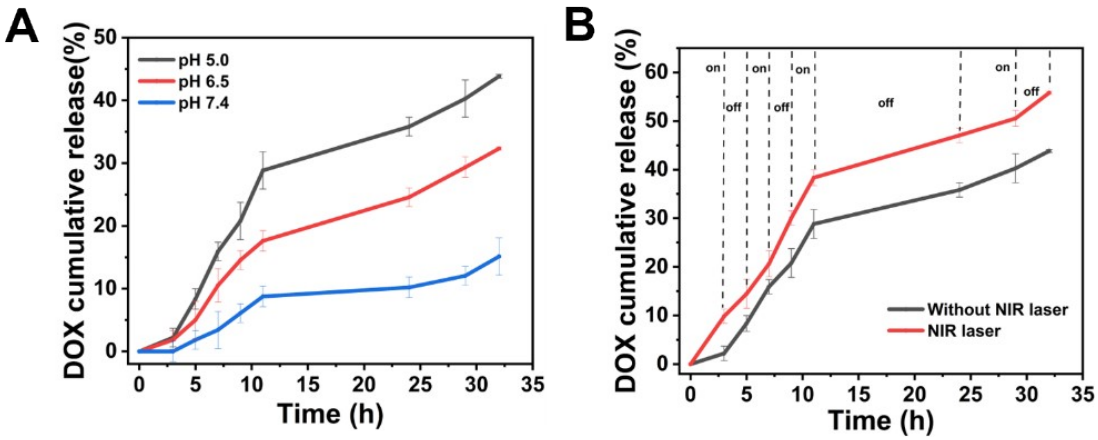

Fig. S19. (A) Cumulative release of DOX from LAKDFeD at different pH values (7.4, 6.5 and 5.0). (B) Effect of NIR irradiation on the release of DOX from LAKDFeD. NIR laser: 808 nm, 1.0 W/cm^2, and 8 min for irradiation duration.

17. The effect of pH on the catalytic oxidation of TMB by LAKDCu and LAKDFe

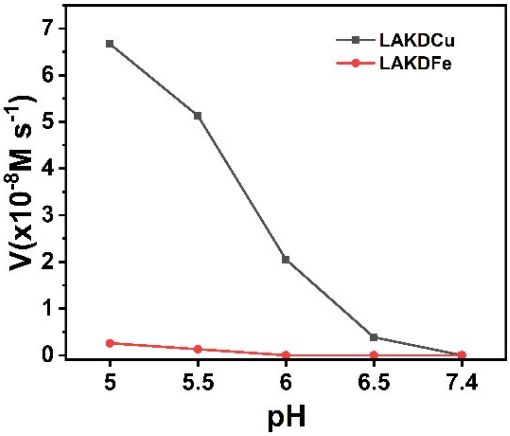

Fig. S20. The effect of pH on the catalytic oxidation of TMB by LAKDCu and LAKDFe.

18. The effects of LAKDCu concentrations and reaction temperatures on the catalytic

oxidation of GSH by LAKDCu

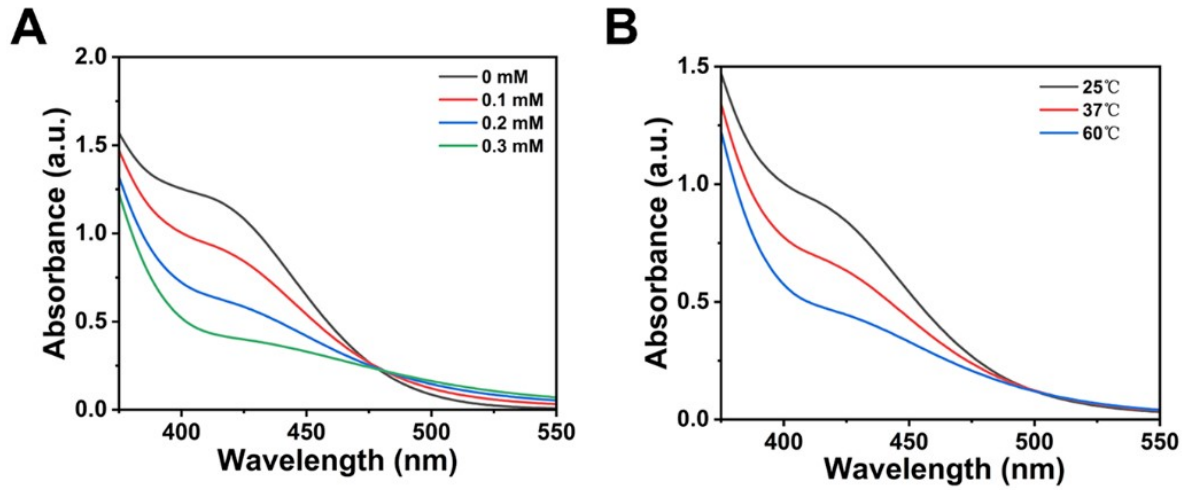

Fig. S21. The effect of LAKDCu concentrations (A) and reaction temperatures (B) on the catalytic oxidation of GSH.

19. Flow cytometry analysis of 4T1 cells treated by free DOX and LAKDCuD for 3 and 6 h

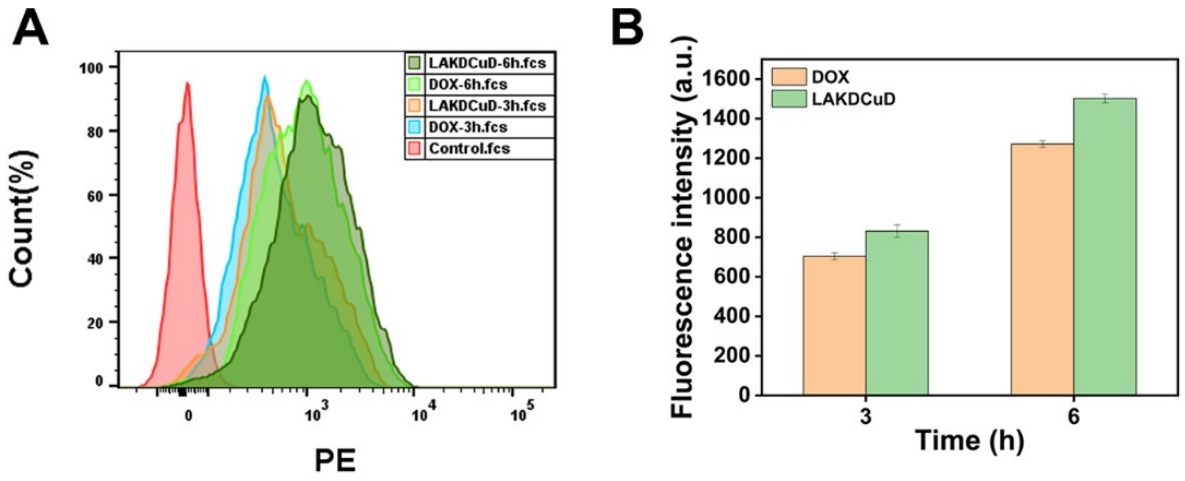

Fig. S22. Fluorescence intensities of 4T1 cells treated by DOX and LAKDCuD for 3 and 6 h.

20. Flow cytometric analysis of 4T1 cells stained by DCFH-DA

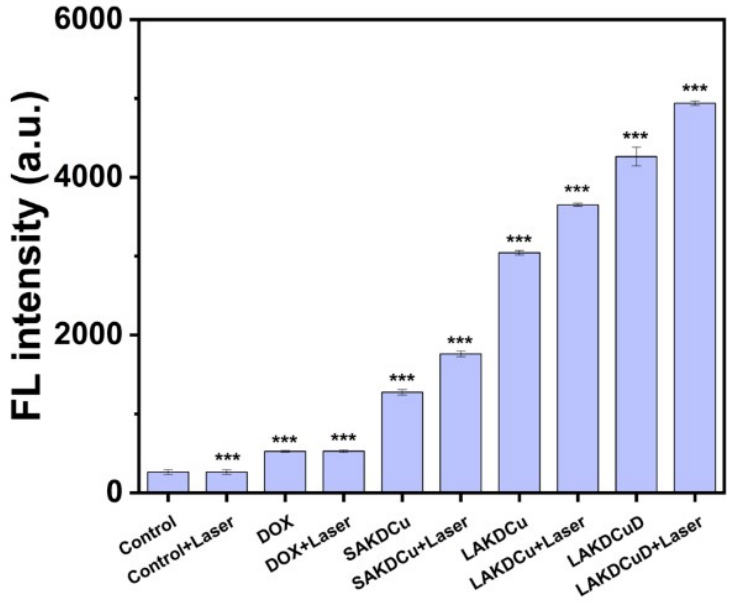

Fig. S23. Flow cytometric analysis of intracellular ROS levels in 4T1 cells treated by PBS, DOX, SAKDCu, LAKDCu, and LAKDCuD, together with 808 nm laser irradiation (1.0 W/cm²). Data were shown as mean ± SD (n = 3), *p<0.05, **p<0.01 and ***p<0.001.

21. Flow cytometric analysis of intracellular GSH levels in 4T1 cells

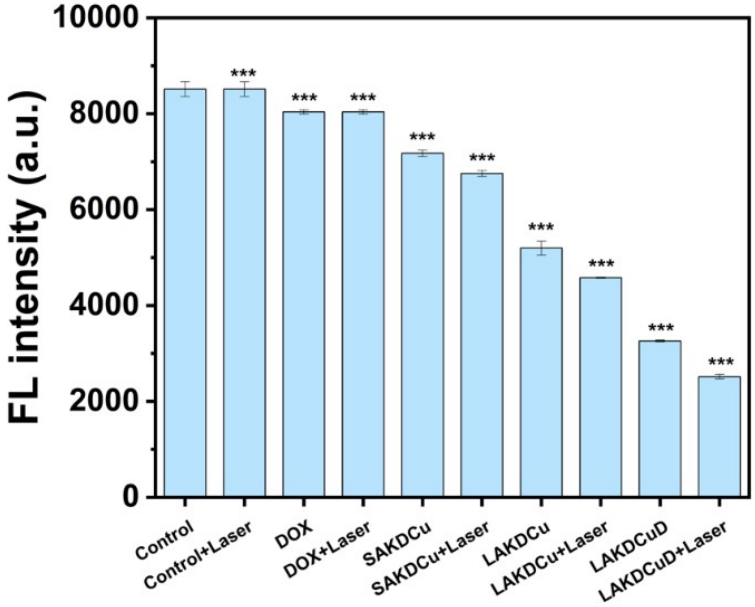

Fig. S24. Flow cytometric analysis of intracellular GSH levels in 4T1 cells treated by PBS, DOX, SAKDCu, LAKDCu, and LAKDCuD, together with 808 nm laser irradiation (1.0 W/cm²). Data were shown as mean ± SD (n = 3), *p<0.05, **p<0.01 and ***p<0.001.

22. Cell viabilities of HUVEC and L929 cells co-cultured with SAKDCu and LAKDCu for 24 h

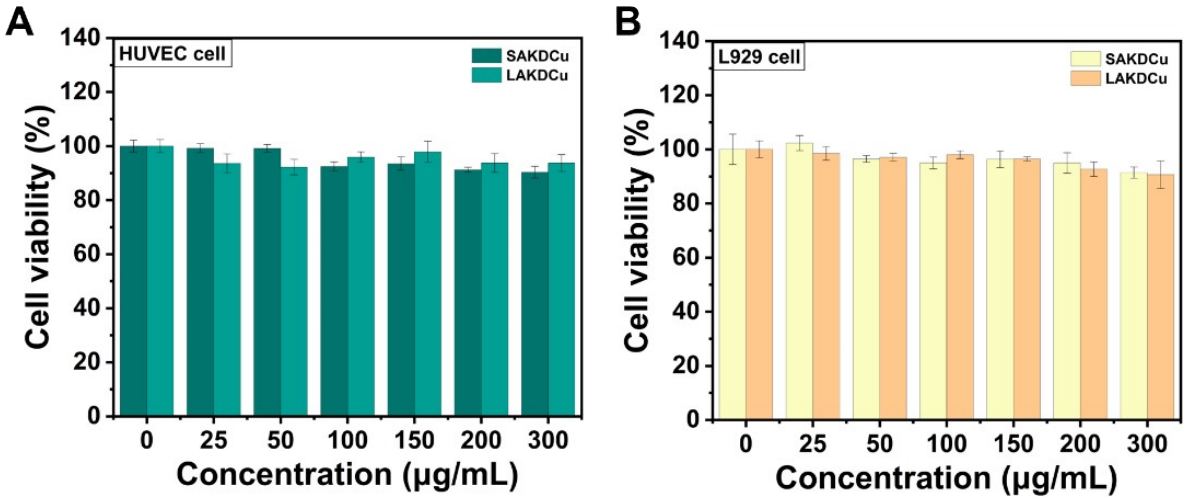

Fig. S25. Relative cell viabilities of (A) HUVEC and (B) L929 cells incubated with different concentrations of SAKDCu and LAKDCu (0, 25, 50, 100, 150, 200 and 300 μg/mL) for 24 h.

23. Viabilities of 4T1 cells treated by varied amounts of DOX and LAKDCuD

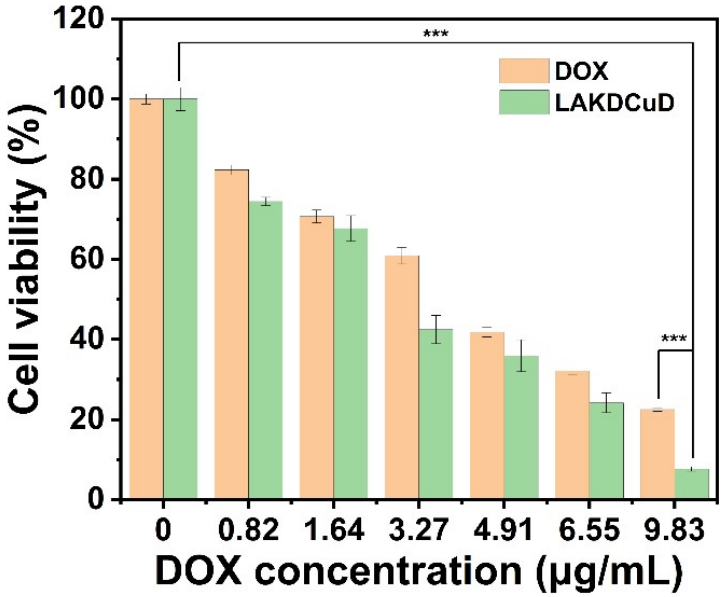

Fig. S26. Viabilities of 4T1 cells treated by varied amounts of DOX and LAKDCuD (at the same DOX-equivalent concentration) for 24 h. Data were shown as mean ± SD (n = 3), *p<0.05, **p<0.01 and ***p<0.001.

24. Cell viability of 4T1 cells co-treated with LAKDCu and ferrostatin-1 for 24 h

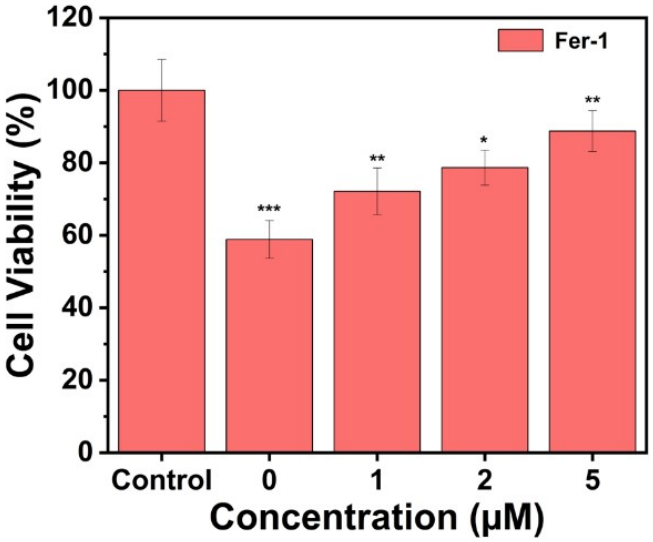

Fig. S27. Cell viability of 4T1 cells co-treated with LAKDCu (100 μg /mL) and ferrostatin-1 in different concentrations (1, 2 and 5 μM) for 24 h. Data were shown as mean ± SD (n = 3), *p<0.05, **p<0.01 and ***p<0.001.